BNL-114734-2017-JAAM

0D-2D and 1D-2D semiconductor hybrids composed of all inorganic perovskite nanocrystals and single layer graphene with improved light harvesting

M. Cotlet,

To be published in "Particle and Particle Systems Characterization"

November 2017

Center for Functional Nanomaterials

Brookhaven National Laboratory

U.S. Department of Energy

USDOE Office of Science (SC),

USDOE Office of Science (SC), Basic Energy Sciences (BES) (SC-22)

Notice: This manuscript has been authored by employees of Brookhaven Science Associates, LLC under Contract No. DE-SC0012704 with the U.S. Department of Energy. The publisher by accepting the manuscript for publication acknowledges that the United States Government retains a non-exclusive, paid-up, irrevocable, world-wide license to publish or reproduce the published form of this manuscript, or allow others to do so, for United States Government purposes.

DISCLAIMER

This report was prepared as an account of work sponsored by an agency of the United States Government. Neither the United States Government nor any agency thereof, nor any of their employees, nor any of their contractors, subcontractors, or their employees, makes any warranty, express or implied, or assumes any legal liability or responsibility for the accuracy, completeness, or any third party's use or the results of such use of any information, apparatus, product, or process disclosed, or represents that its use would not infringe privately owned rights. Reference herein to any specific commercial product, process, or service by trade name, trademark, manufacturer, or otherwise, does not necessarily constitute or imply its endorsement, recommendation, or favoring by the United States Government or any agency thereof or its contractors or subcontractors. The views and opinions of authors expressed herein do not necessarily state or reflect those of the United States Government or any agency thereof.

BNL- 114734 -2017-JA

0D-2D and 1D-2D semiconductor hybrids composed of all inorganic perovskite nanocrystals and single layer graphene with improved light harvesting

Jia-Shiang Chen, Tennyson L. Doane, Mingxing Li, Huidong Zang, Mathew M. Maye, and Mircea Cotlet

Submitted to Particle and Particle Systems Characterization

November 2017

Center for Functional Nanomaterials

Brookhaven National Laboratory

U.S. Department of Energy
USDOE Office of Science (SC),
Basic Energy Sciences (SC-22)

Notice: This manuscript has been authored by employees of Brookhaven Science Associates, LLC under Contract No. DE- SC0012704 with the U.S. Department of Energy. The publisher by accepting the manuscript for publication acknowledges that the United States Government retains a non-exclusive, paid-up, irrevocable, world-wide license to publish or reproduce the published form of this manuscript, or allow others to do so, for United States Government purposes.

DISCLAIMER

This report was prepared as an account of work sponsored by an agency of the United States Government. Neither the United States Government nor any agency thereof, nor any of their employees, nor any of their contractors, subcontractors, or their employees, makes any warranty, express or implied, or assumes any legal liability or responsibility for the accuracy, completeness, or any third party's use or the results of such use of any information, apparatus, product, or process disclosed, or represents that its use would not infringe privately owned rights. Reference herein to any specific commercial product, process, or service by trade name, trademark, manufacturer, or otherwise, does not necessarily constitute or imply its endorsement, recommendation, or favoring by the United States Government or any agency thereof or its contractors or subcontractors. The views and opinions of authors expressed herein do not necessarily state or reflect those of the United States Government or any agency thereof.

DOI: 10.1002/ ((ppsc.201700310R1))

Article type: Full Paper

0D-2D and 1D-2D semiconductor hybrids composed of all inorganic perovskite nanocrystals and single layer graphene with improved light harvesting

Jia-Shiang Chen,[1,2] Tennyson L. Doane,[3] Mingxing Li,[1] Huidong Zang,[1] Mathew M. Maye,[3] and Mircea Cotlet[1*]*

Jia-Shiang Chen,[1,2], Dr. Mingxing Li,[1] Dr. Huidong Zang,[1] and Dr. Mircea Cotlet[1*]
[1]Center for Functional Nanomaterials, Brookhaven National Laboratory, Upton, NY 11973, USA and [2]Department of Materials Science and Chemical Engineering, Stony Brook University, Stony Brook, NY 11794, USA
E-mail: cotlet@bnl.gov

Dr. Tennyson L. Doane and Prof. Dr. Mathew M. Maye
[3]Department of Chemistry, Syracuse University, Syracuse, NY 13244, USA
E-mail: mmmaye@syr.edu

Keywords: perovskite nanocrystals and nanowires, single layer graphene, electron transfer, single nanocrystal spectroscopy, blinking

Abstract. In this study, we combined all inorganic cesium lead iodide (CsPbI3) perovskite nanoparticles (PNPs) and perovskite nanowires (PNWs) with single layer graphene (SLG) to obtain 0D-2D PNP-SLG and 1D-2D PNW-SLG hybrids with improved light harvesting. Time-resolved single nanostructure photoluminescence studies of PNPs, PNWs and related hybrids revealed (i) quasi two-state photoluminescence blinking in PNPs, (ii) highly polarized photoluminescence emitted by PNWs and (iii) efficient interfacial electron transfer between perovskite nanostructures and SLG in both PNP-SLG and PNW-SLG hybrids. Doping of poorly absorbing, highly conductive single layer graphene with perovskite nanocrystals and nanowires provides a simple, yet efficient path to obtain hybrids with increased light harvesting properties for potential utilization in the next generation photodetectors and photovoltaic devices, including polarization sensitive photodetectors.

1. Introduction

Two-dimensional (2D) layered materials such as graphene and layered metal dichalcogenides like MoS_2, WS_2, SnS_2, etc., have attracted considerable interest due to their intrigue and unique physical properties which are connected with their low dimensionality,

which in turn provides appealing properties for photovoltaics, photodetectors, catalysis or for chemical and biological sensors.[1] Single layer graphene (SLG), a prevalent 2D carbon material, maintains both metallic and semiconducting properties and it has been proposed as electron acceptor and conductor layer or as a photodetector due to its spectrally broad and ultrafast response.[1c, 1d] However, as a single-atom-thick layer, graphene is inherently poor in absorbing light, exhibiting about 2-2.3% absorbance.[2] One way to improve light harvesting of atomically thin 2D materials is to dope them with zero dimensional (0D) quantum dots (QDs).[3] Such 0D-2D hybrids have been found to exhibit improved photoresponse and higher performance in modern optoelectronic devices [1e, 1f, 3a, 3b, 3e-h, 4]. 0D-2D hybrids have been demonstrated mostly with II-VI semiconducting QDs and improvement in photoresponse in such hybrids was achieved either by photoinduced charge transfer[4a, 5] or by nonradiative energy transfer[3f-h] between 0D and 2D components.

Here we report 0D-2D and 1D-2D hybrids based on all inorganic cesium lead-halide nanoparticles and nanowires and SLG (see **Figure 1**a and 1b for conceptual drawings of hybrids). Colloidal nanoparticles based on all-inorganic cesium lead-halide ($CsPbX_3$, X = Cl^-, Br^-, I^-,) perovskites, or PNPs, are a new class of nanomaterials with great potential for solid state lightening, photovoltaics and photodetector applications.[7] PNPs exhibit the benefits of size tunable optical and electronic properties found in II-VI semiconducting QDs[8], with band engineering achieved by alteration of the composition of different halides of $CsPbX_3$.[7a-e] Among various $CsPbX_3$, red emitting $CsPbI_3$ PNPs exhibit the longest carrier recombination lifetime[7k], high quantum yield of photoluminescence and absorption spanning the entire UV-VIS spectral range, properties which make them not only great light harvesting nanomaterials but also strong candidates for single nanocrystal photoluminescence (PL) studies, including those involving quenching by energy and charge transfer.[3d, 4b, 6, 9] Here we assembled and characterized spectroscopically two types of graphene-perovskite nanocrystal hybrids: (i) 0D-2D nanohybrids based on SLG doped with $CsPbI_3$ PNPs (hereafter named PNP-SLG

nanohybrids) and (ii) 1D-2D nanohybrids based on SLG doped with perovskite nanowires (PNWs), with PNWs self-assembled from $CsPbI_3$ PNPs (hereafter named PNW-SLG nanohybrids). We used time resolved single nanocrystal photoluminescence spectroscopy to unveil the mechanism of emission in both PNPs and PNWs and the interfacial interaction mechanism in PNP-SLG and PNW-SLG nanohybrids.

2. Results and discussions

2.1. Perovskite nanoparticles (PNPs)

Colloidal $CsPbI_3$ PNPs capped with oleylammonium halide and oleylammonium oleate and dissolved in hexane were synthesized following a method reported by Kovalenko *et al.* [7c, 7d] They are cubic (≈10nm size on average) as presented by the transmission electron microscopy (TEM) (Jeol 1400) image inset shown in Figure 1c and as previously reported.[7k] Absorption and photoluminescence (PL) spectra are shown in Figure 1c, with the PL spectrum featuring a single peak at 684 nm (full width at half maximum, FWHM of 35 nm). PNPs in hexane emit with a PL quantum yield of about 46% and an average ensemble PL decay time of 21.4 ns (see SI for details on calculations of PL quantum yield and decay time). Highly diluted PNPs in hexane were spincasted on Piranha cleaned cover glasses under argon atmosphere to yield a coverage of one nanoparticle per 4 μm^2 or lower, a concentration suitable for single nanocrystal imaging. Samples were transferred onto a sealed holder for confocal photoluminescence lifetime imaging (FLIM), with FLIM images acquired with a 440nm pulsed laser excitation source of 10 MHz repetition rate and 90 ps pulse width (Picoquant Germany) using an average power of 100nW at the sample. FLIM images were acquired with a single photon counting avalanche photodiode (Micro Photon Devices, 45 ps response) by sending the collected PL signal through a 532nm dichroic mirror (Semrock), a 75μm confocal pinhole and a 632nm long pass filter (Semrock). A detailed description of the confocal FLIM can be found in reference.[3f] For the laser excitation conditions used by us, the average number of excitation photons per PNP is $\langle N \rangle = \frac{\sigma \times P_{exc}}{h\nu_{exc} \times d \times \Omega_{exc}} = 0.05$ and probability of biexciton formation is $P(2) = \frac{<N>^2 e^{-<N>}}{2} << 0.1$, so that pulsed excitation of isolated PNPs produced mainly single electron-hole pairs.[7f, 10] Here σ is the absorption cross section of PNPs[7f], P_{exc}, $h\nu_{exc}$ and

Ω_{exc} are the laser power, photon energy and repetition rate, respectively and d is the laser spot size at the sample (Olympus oil immersion lens, 1.4 NA, 100x magnification).

A confocal FLIM image recorded from isolated PNPs on glass is shown in **Figure 2**a and it already evidences blinking or on/off switching of the PL emitted by these PNPs while imaging by sample raster scanning. Figure 2b shows the time-resolved PL decay trace recorded from a single PNP on glass and it has an average PL decay time τ_{PNP}=13.36 ns, similar to previous single nanocrystal PL reports.[7f] Blinking validates the probing of isolated PNPs and this phenomenon is better seen in the PL intensity vs time trajectory in Figure 2c, and its zoom in Figure 2d. The photon counting histogram in Figure 2d (black color) derived from the PL trajectory in Figure 2c (black color) distinguishes two intensity levels, a well-defined "off-state" and a "quasi on-state" of large width. In colloidal II-VI quantum dots like CdSe/ZnS the on-state is usually of constant amplitude[11]. Time-resolved PL data recorded from several (15) isolated $CsPbI_3$ PNPs on glass were used to construct a probability density distribution of PL lifetimes (**Figure 3**a), which fitted with a Gauss model (OriginPro 8.5), rendered a mean PL decay time τ_{PNP}=15.2 ns ($FWHM_{PNP}$=9.9 ns). Details on how these distributions were constructed are given in supplementary information (SI). The change in PL lifetime from solution (hexane) to glass could be related to changes in the dielectric constant from solvent to glass (ε_{hexane}=1.9 vs ε_{glass}=3.8).

We now return to the PL blinking of single $CsPbI_3$ PNPs on glass. We analyzed PL intensity traces like those shown in Figure 2c (black color) for several (15) PNPs by using a threshold method[11b, 12] which discriminates between on-times (emissive state or on-state) and off-times (non-emissive state or off-state). "Ensemble-like" probability distributions for on-times ($P(t_{on})$) and off-times ($P(t_{off})$) are shown in **Figures 4**a and 4b (black color). Fits according to a power law model $P(t_i) = b \times t^{-m_i}$, with i=*on; off*, b a constant and m_i power law exponent yielded m_{on}(PNP)=1.46 and m_{off}(PNP)=1.82 (Table 1), values which are in the range of those reported for II-VI semiconductor QDs,[11a] thus reconfirming the universality of PL blinking among various types of semiconductor quantum dots. For II-VI semiconductor QDs like CdSe, blinking has been related to photocharging and neutralization of QD's core following optical excitation.[13] An emissive (on-) state will result from radiative recombination of the

photogenerated electron-hole pair and a dark (off-) state will result from charge trapping of either photogenerated electron or hole outside the core followed by trion formation and efficient non-radiative Auger recombination in the QD core. A charged QD may become neutral and capable of emitting photoluminescence if it undergoes charge recombination between the remaining charge in the core and the opposite charge trapped outside. A similar scenario which takes into consideration photocharging of the PNP and an involvement of surface charge traps has been proposed for $CsPbX_3$ PNPs and for some organic-inorganic PNPs.[7g, 7j, 14]

2.2. Perovskite nanowires (PNWs).

Colloidal $CsPbX_3$ perovskites nanowires have already been reported via solution-phase synthesis or ultrasonication-assisted synthesis.[15] In our study, PNWs were assembled from freshly synthesized perovskite nanoparticles by heating them in solution at 100°C for 1 hour and then for another 1 hour at 140°C, followed by purification by centrifugation (6000 RPM for 5 minutes). Figure 1d shows as inset a TEM image highlighting the formation of PNWs of ≈1.1 μm length and 50 nm width, with several single nanowires forming a bundle. We observed PNWs of various lengths by TEM imaging in the 0.6~1.4 μm range. Additional TEM images are shown in Figure S2, SI. Moreover, TEM images of PNPs from early stage synthesis shown in Figure S3, indicating oriented-attachment mechanism of PNWs' formation.[15c] PNWs photoluminescence spectra are blue shifted, single band, with a peak at 670 nm (FWHM 38 nm). Correlative confocal FLIM and back scattering reflection images of a single PNW are shown in Figure 5a and 5b. The reflection image identifies the PNW based on its micron size length. Photoluminescence recorded from the isolated PNW does not exhibit blinking, but rather exhibits fluctuating PL intensity (Figure 5c). PL lifetime is highly heterogeneous among various PNWs as can be seen from Figure 3b, where the black colored histogram represents the probability density distribution of PL lifetimes calculated from several isolated PNWs (see SI for details on PL lifetime calculations and Table 1, with mean value of distribution τ_{PNW}=7.7

ns, FWHM=4.05 ns). PNW's PL lifetime is heterogeneous also within a single PNW, as shown by the confocal FLIM image in Figure 5a where the inner region of the PNW is quenched (<τ_{PNW}(region2)>=2.4ns) compared to the side regions (<τ_{PNW}(region1)>=3.9ns). Therefore, the overall PL decay from an isolated PNP features usually a multiexponential decay profile (Figure 5d, black color).

We performed photoluminescence polarization modulation experiments on PNPs and PNWs. In these experiments, an isolated nanostructure, PNP or PNW, was excited with linear polarized laser excitation having the polarization direction constantly changed (10 degree/sec controlled by motorized rotation stage with a λ/2 waveplate), while the laser intensity was kept constant and the emitted PL was recorded. If a transition dipole moment existed in the nanostructure, this could be revealed through the modulated PL response of the nanostructure. For isolated PNWs, we observed polarization modulation of the emitted PL, mainly at the center of the PNW (Figure 5e) and almost no modulation at both PNW's sides. We estimated a photoluminescence polarization P= $I_{\parallel} - I_{\perp} / I_{\parallel} + I_{\perp} = 0.62$, with $I_{\parallel}$ and $I_{\perp}$ the parallel and perpendicular PL polarized signals, respectively, which here correspond to the lowest and highest PL intensities observed in the modulated trace in Figure 5e. Polarization modulation in inorganic nanowires has been observed previously and it has been associated with sharp dielectric contrast at the nanowire-surrounding interface, a property which could be exploited to create polarization-sensitive photodetectors.[16] In contrast, isolated PNP did not show any response to polarization modulation (Figure 5f), evidencing that a preferential transition dipole moment does not exists, similar to II-VI semiconductor quantum dots which exhibit a spherically degenerated transition dipole.[17] In a recent study,[18] highly polarized emission was reported for $CsPbX_3$ quantum dots in solution and thin film, including $CsPbI_3$. Those authors argued that such polarized emission from $CsPbX_3$ quantum dots might result from the unique cubic crystal structure of perovskites or from large area, well aligned clusters of these quantum

dots. Our polarization data for $CsPbI_3$ nanoparticles clearly indicate that no polarization is present in perovskite nanoparticles, therefore no relation exists between their cubic structure and a preferential direction for their transition dipole moment. Instead, such polarized emission comes from aggregates, in our case nanowires. We also did not observe lasing as reported for other perovskite nanowires[19], and we believe the reason for this is the absence of flat end facets in the case of our wires which prevents formation of optical resonator cavities (see Figure 1d and Figure S2, SI). These same imperfections might also explain why our PNWs, when excited at sides, do not show a modulated response in PL following polarization modulation excitation.

2.3. 0D-2D PNP-SLG hybrids.

We deposited diluted PNPs on SLG. The SLG was grown by chemical vapor deposition on glass (Graphene Supermarket Inc.) and confirmed by us as a single layer with confocal Raman microspectroscopy (Figure S1, SI) with characteristic Raman bands G and 2D identified at 1578 and 2668 cm^{-1}, respectively. According to the manufacturer, SLG was of n–type doping. We observed significant PL quenching of PNPs on SLG. The PL decay shown in red in Figure 2b was recorded from an isolated PNP on SLG and it has an average PL lifetime $\tau_{PNP-SLG}$= 4.82 ns, about three times quenched than in the case of PNPs on glass (Figure 2b, black curve). Time-resolved PL measurements were performed on several (13) PNPs on SLG to build the probability density of PL lifetimes shown in Figure 3a (grey color). This distribution, when fit with a Gauss function, it exhibited a mean PL lifetime $\tau_{PNP-SLG}$= 5.54ns and a $FWHM_{PNP\text{-}SLG}$= 4.2 ns. With these mean PL lifetime values (Table 1) we estimated a quenching rate $\eta_{quench}^{PNP-SLG} = {}^{1}/_{\tau_{PNP}} - {}^{1}/_{\tau_{PNP-SLG}}$ =1.14x$10^8 s^{-1}$ and a quenching efficiency $E_{PNP-SLG} = 1 - {}^{\tau_{PNP-SLG}}/_{\tau_{PnP}}$= 64%. Quenching of PL emitted by II-IV semiconducting QDs by single layer graphene has been previously associated with either nonradiative energy transfer[3d, 3e, 20] or with photoinduced charge transfer[21] between photoexcited QDs and SLG. Both energy and charge transfer reduce the PL intensity and PL lifetime of a QD when compared to its value on a neutral

support. Changes in radiative recombination rate when going from glass substrate to SLG can also produce changes in PL intensity and PL lifetime, but these usually feature anti correlated PL intensity vs PL lifetime behavior[20], opposite to what we observed for PNPs. Energy transfer is possible because of the overlap of SLG's absorption and PNP's emission (Figure 1c) and because of the close proximity of the two nanomaterials, here about the length of the PNP ligand (oleylammonium oleate, ~2.2nm). The energy band alignment between PNP's conduction band (CB) and SLG's Fermi level, with n-type SLG, favors also photoinduced electron transfer from PNP to SLG. This last process is more likely to outscore energy transfer because of the very low exciton binding energy of $CsPbI_3$ PNP (20 meV according to reference[7i]) which favors electron extraction by n-type SLG following optical excitation rather than exciton transfer by energy transfer (Figure 1e). Colloidal II-VI semiconductor QDs undergoing energy transfer with SLG reported in reference[3d] were core/shell CdSe/ZnS with exciton binding energies in CdSe in the range of 200-1000meV[22] and with the ZnS shell being a high bandgap energy material and acting as a tunneling barrier towards possible charge transfer.

Single nanocrystal PL spectroscopy can discriminate between interfacial energy transfer and charge transfer in QD-based hybrids by monitoring changes in the PL blinking of photoexcited QDs in the presence/absence of an external acceptor.[3f] We recall that PL blinking in colloidal II-VI semiconductor QDs relates to photocharging/neutralization of QD's core following optical excitation and that it involves surface defects acting as charge traps of photogenerated charges.[11a, 23] If a photoexcited QD undergoes charge transfer with an external acceptor, this will compete with the internal charge trapping process, influencing the energetics and the lifetime of the surface charge trap, and this in turn will change the dynamics of the PL blinking. Changes in the dynamics of PL blinking of QDs in interaction with external charge acceptors have been reported, mainly for 0D-0D hybrids based on CdSe/ZnS QDs.[11b, 12a, 24] If a photoexcited QD undergoes nonradiative energy transfer with an external acceptor, no photogenerated single changes are exchanged between the donor (QD) and acceptor, but only

excitons, therefore no changes in PL blinking are observed.[3f] The on-time ($P_{on}(t)$) and off-time ($P_{off}(t)$) probabilities for PNPs on SLG are shown in Figure 4a and 4b (red color). When fit with a power law model, $P_{on}(t)$ for PNPs on SLG feature an increase in on-time power law exponent compared to glass, m_{on}(PNP-SLG)=1.62 vs m_{on}(PNP)=1.46 (Table 1), reflecting the decrease in on-time or emissive time due to the introduction of external electron transfer as a new quenching path next to internal charge trapping. $P_{off}(t)$ for PNPs on SLG feature a decrease in power law exponent compared to glass, m_{off}(PNP-SLG)=1.67 vs m_{on}(PNP)=1.82 (Table 1), reflecting the increase in off-time or dark time due to the introduction of external electron recombination as an additional step in the PNP neutralization path. As such, single nanocrystal experiments reported here classify the interfacial interaction mechanism between PNPs and SLG as electron transfer.

2.4. 1D-2D PNW-SLG hybrids.

As with the PNP-SLG hybrid, the PNW-SLG will also exhibit interfacial electron transfer following photoexcitation of the PNWs given their energy band alignment which is similar to that of PNPs (Figure 1, see PL spectra of PNPs and PNWs) and allowing electron transfer with SLG. To test this hypothesis, we deposited diluted PNWs on single layer graphene to obtain 1D-2D PNW-SLG hybrids for which we observed strong PL quenching, stronger than for 0D-2D PNP-SLG hybrids. Figure 5c and 5d, red colors, show PL intensity vs time trajectories and PL decays from a PNW on SLG, which confirms graphene induces strong PL quenching. Figure 3b (red color) contains a probability distribution histogram of PL lifetimes estimated from several PNWs deposited on SLG which has a mean value $\tau_{PNW-SLG}$= 1.58 ns and a width $FWHM_{PNW\text{-}SLG}$=0.95 ns (see SI for PL lifetime calculations). The rate and the efficiency for this quenching process are $k_{ET}^{PNW-SLG} = {}^{1}/_{\tau_{PNW}} - {}^{1}/_{\tau_{PNW-SLG}}$=5.06x$10^{8}s^{-1}$ and $E_{PNW-SLG} = 1 - {}^{\tau_{PNW-SLG}}/_{\tau_{PNW}}$= 79%. The reason why PNWs are quenched stronger by

SLG than PNPs is not yet clear to us but we speculate that the strong dipole created in the PNWs might play a role.

3. Conclusion

In summary, we reported single nanocrystal photoluminescence experiments on $CsPbI_3$ perovskite nanocrystals (PNPs), newly synthesized perovskite nanowires (PNWs) and their 0D-2D and 1D-2D hybrids with single layer graphene. We found isolated PNPs to exhibit photoluminescence emission, including two-state blinking dynamics, similar to colloidal II-VI semiconductor quantum dots, reconfirming the universality of blinking across many types of semiconducting nanocrystals. PNWs with micron sized length and high (20:1) aspect ratio were synthesized following a thermal approach and were also investigated with single nanocrystal PL spectroscopy and found to emit highly polarized photoluminescence as a result of sharp dielectric contrast at the nanowire-surrounding interface. For PNP-SLG hybrids, an analysis of the PL blinking helped us to unveil electron transfer as the interfacial interaction mechanism occurring in these hybrids. Both PNP-SLG and PNW-SLG hybrids exhibited strong interfacial electron transfer interactions, with perovskite nanostructures aiding to the light harvesting properties of SLG for potential detector implementation of such hybrids. Furthermore, the polarized emission of PNWs could be exploited in the future for polarization sensitive detectors based on PNW-SLG hybrids. Doping of poorly absorbing, highly conductive SLG with PNPs and PNWs provides a simple, yet efficient path to obtain hybrids with increased light harvesting properties and improved exciton generation, making these hybrids appealing low dimensional semiconductor nanomaterials for next generation photodetector devices.

Supporting Information

Supporting Information is available from the Wiley Online Library or from the author.

Acknowledgements

This work was carried out in part at the Center for Functional Nanomaterials, Brookhaven National Laboratory (BNL), which is supported by the U.S. Department of Energy, Office of Basic Energy Sciences, under Contract No. DE-SC0012704.

[1] a) Y. Huang, E. Sutter, J. T. Sadowski, M. Cotlet, O. L. A. Monti, D. A. Racke, M. R. Neupane, D. Wickramaratne, R. K. Lake, B. A. Parkinson, P. Sutter, *ACS Nano* **2014**, 8, 10743; b) A. Splendiani, L. Sun, Y. Zhang, T. Li, J. Kim, C. Y. Chim, G. Galli, F. Wang, *Nano Lett* **2010**, 10, 1271; c) X. Gan, R.-J. Shiue, Y. Gao, I. Meric, T. F. Heinz, K. Shepard, J. Hone, S. Assefa, D. Englund, *Nature Photonics* **2013**, 7, 883; d) C. H. Liu, Y. C. Chang, T. B. Norris, Z. Zhong, *Nat Nanotechnol* **2014**, 9, 273; e) C. X. Guo, H. B. Yang, Z. M. Sheng, Z. S. Lu, Q. L. Song, C. M. Li, *Angew Chem Int Ed Engl* **2010**, 49, 3014; f) Y. Huang, H. Zang, J.-S. Chen, E. A. Sutter, P. W. Sutter, C.-Y. Nam, M. Cotlet, *Applied Physics Letters* **2016**, 108, 123502.

[2] K. F. Mak, L. Ju, F. Wang, T. F. Heinz, *Solid State Communications* **2012**, 152, 1341.

[3] a) Y. Gromova, A. Alaferdov, S. Rackauskas, V. Ermakov, A. Orlova, V. Maslov, S. Moshkalev, A. Baranov, A. Fedorov, *Journal of Applied Physics* **2015**, 118, 104305; b) G. Konstantatos, M. Badioli, L. Gaudreau, J. Osmond, M. Bernechea, F. P. Garcia de Arquer, F. Gatti, F. H. Koppens, *Nat Nanotechnol* **2012**, 7, 363; c) J. Liu, P. Kumar, Y. Hu, G. J. Cheng, J. Irudayaraj, *The Journal of Physical Chemistry C* **2015**, 119, 6331; d) Z. Chen, S. Berciaud, C. Nuckolls, T. F. Heinz, L. E. Brus, *ACS Nano* **2010**, 4, 2964; e) O. A. Ajayi, N. C. Anderson, M. Cotlet, N. Petrone, T. Gu, A. Wolcott, F. Gesuele, J. Hone, J. S. Owen, C. W. Wong, *Applied Physics Letters* **2014**, 104, 171101; f) H. Zang, P. K. Routh, Y. Huang, J. S. Chen, E. Sutter, P. Sutter, M. Cotlet, *ACS Nano* **2016**, DOI: 10.1021/acsnano.6b01538; g) F. Prins, A. J. Goodman, W. A. Tisdale, *Nano Lett* **2014**, 14, 6087; h) A. Raja, A. Montoya Castillo, J. Zultak, X. X. Zhang, Z. Ye, C. Roquelet, D. A. Chenet, A. M. van der Zande, P. Huang, S. Jockusch, J. Hone, D. R. Reichman, L. E. Brus, T. F. Heinz, *Nano Lett* **2016**, 16, 2328.

[4] a) D. Kufer, I. Nikitskiy, T. Lasanta, G. Navickaite, F. H. L. Koppens, G. Konstantatos, *Advanced Materials* **2015**, 27, 176; b) D.-H. Kwak, D.-H. Lim, H.-S. Ra, P. Ramasamy, J.-S. Lee, *RSC Advances* **2016**, 6, 65252.

[5] B.-S. Kim, D. C. J. Neo, B. Hou, J. B. Park, Y. Cho, N. Zhang, J. Hong, S. Pak, S. Lee, J. I. Sohn, H. E. Assender, A. A. R. Watt, S. Cha, J. M. Kim, *ACS Applied Materials & Interfaces* **2016**, 8, 13902.

[6] Y.-F. Xu, M.-Z. Yang, B.-X. Chen, X.-D. Wang, H.-Y. Chen, D.-B. Kuang, C.-Y. Su, *Journal of the American Chemical Society* **2017**, 139, 5660.

[7] a) P. Ramasamy, D. H. Lim, B. Kim, S. H. Lee, M. S. Lee, J. S. Lee, *Chem Commun (Camb)* **2016**, 52, 2067; b) X. Li, Y. Wu, S. Zhang, B. Cai, Y. Gu, J. Song, H. Zeng, *Advanced Functional Materials* **2016**, 26, 2435; c) L. Protesescu, S. Yakunin, M. I. Bodnarchuk, F. Krieg, R. Caputo, C. H. Hendon, R. X. Yang, A. Walsh, M. V. Kovalenko, *Nano Lett* **2015**, 15, 3692; d) G. Nedelcu, L. Protesescu, S. Yakunin, M. I. Bodnarchuk, M. J. Grotevent, M. V. Kovalenko, *Nano Lett* **2015**, 15, 5635; e) Q. A. Akkerman, V. DInnocenzo, S. Accornero, A. Scarpellini, A. Petrozza, M. Prato, L. Manna, *J Am Chem Soc* **2015**, 137, 10276; f) Y.-S. Park, S. Guo, N. S. Makarov, V. I. Klimov, *ACS Nano* **2015**, 9, 10386; g) N. S. Makarov, S. Guo, O. Isaienko, W. Liu, I. Robel, V. I. Klimov, *Nano Lett* **2016**, 16, 2349; h) F. Hu, H. Zhang, C. Sun, C. Yin, B. Lv, C. Zhang, W. W. Yu, X. Wang, Y. Zhang, M. Xiao, *ACS Nano* **2015**, 9, 12410; i) A. Swarnkar, R. Chulliyil, V. K. Ravi, M. Irfanullah, A. Chowdhury, A. Nag, *Angew Chem Int Ed Engl* **2015**, 54, 15424; j) S. Seth, N. Mondal, S. Patra, A. Samanta, *J Phys Chem Lett* **2016**, 7, 266; k) T. L. Doane, K. L. Ryan, L. Pathade, K. J. Cruz, H. Zang, M. Cotlet, M. M. Maye, *ACS Nano* **2016**, DOI: 10.1021/acsnano.6b00806; l) A. Swarnkar, A. R. Marshall, E. M. Sanehira, B. D. Chernomordik, D. T. Moore, J. A. Christians, T. Chakrabarti, J. M. Luther, *Science* **2016**, 354, 92.

[8] a) B. O. Dabbousi, J. Rodriguez-Viejo, F. V. Mikulec, J. R. Heine, H. Mattoussi, R. Ober,

K. F. Jensen, M. G. Bawendi, *The Journal of Physical Chemistry B* **1997**, 101, 9463; b) H. Fu, S.-W. Tsang, *Nanoscale* **2012**, 4, 2187.

[9] C. de Weerd, L. Gomez, H. Zhang, W. J. Buma, G. Nedelcu, M. V. Kovalenko, T. Gregorkiewicz, *The Journal of Physical Chemistry C* **2016**, 120, 13310.

[10] J. Zhao, O. Chen, D. B. Strasfeld, M. G. Bawendi, *Nano Letters* **2012**, 12, 4477.

[11] a) M. Kuno, D. P. Fromm, H. F. Hamann, A. Gallagher, D. J. Nesbitt, *The Journal of Chemical Physics* **2001**, 115, 1028; b) Z. Xu, M. Cotlet, *Small* **2012**, 8, 253.

[12] a) S. Jin, T. Lian, *Nano Letters* **2009**, 9, 2448; b) M. Kuno, D. P. Fromm, H. F. Hamann, A. Gallagher, D. J. Nesbitt, *The journal of chemical physics* **2000**, 112, 3117.

[13] M. Nirmal, B. O. Dabbousi, M. G. Bawendi, J. Macklin, *Nature* **1996**, 383, 802.

[14] Y. Tian, A. Merdasa, M. Peter, M. Abdellah, K. Zheng, C. S. Ponseca Jr, T. n. Pullerits, A. Yartsev, V. Sundström, I. G. Scheblykin, *Nano letters* **2015**, 15, 1603.

[15] a) D. Zhang, S. W. Eaton, Y. Yu, L. Dou, P. Yang, *Journal of the American Chemical Society* **2015**, 137, 9230; b) D. Zhang, Y. Yu, Y. Bekenstein, A. B. Wong, A. P. Alivisatos, P. Yang, *Journal of the American Chemical Society* **2016**, 138, 13155; c) Y. Tong, B. J. Bohn, E. Bladt, K. Wang, P. Müller-Buschbaum, S. Bals, A. S. Urban, L. Polavarapu, J. Feldmann, *Angewandte Chemie International Edition*, DOI: 10.1002/anie.201707224n/a.

[16] J. Wang, M. S. Gudiksen, X. Duan, Y. Cui, C. M. Lieber, *Science* **2001**, 293, 1455.

[17] a) D. Patra, I. Gregor, J. Enderlein, M. Sauer, *Applied Physics Letters* **2005**, 87, 101103; b) A. I. Chizhik, A. M. Chizhik, D. Khoptyar, S. Bär, A. J. Meixner, *Nano Letters* **2011**, 11, 1131.

[18] D. Wang, D. Wu, D. Dong, W. Chen, J. Hao, J. Qin, B. Xu, K. Wang, X. Sun, *Nanoscale* **2016**, 8, 11565.

[19] H. Zhu, Y. Fu, F. Meng, X. Wu, Z. Gong, Q. Ding, M. V. Gustafsson, M. T. Trinh, S. Jin, X. Y. Zhu, *Nat Mater* **2015**, 14, 636.

[20] F. Federspiel, G. Froehlicher, M. Nasilowski, S. Pedetti, A. Mahmood, B. Doudin, S. Park, J.-O. Lee, D. Halley, B. Dubertret, *Nano letters* **2015**, 15, 1252.

[21] A. V. Klekachev, I. Asselberghs, S. N. Kuznetsov, M. Cantoro, J. H. Mun, B.-J. Cho, J.-i. Hotta, J. Hofkens, M. van der Veen, A. L. Stesmans, presented at SPIE NanoScience+ Engineering **2012**.

[22] R. W. Meulenberg, J. R. I. Lee, A. Wolcott, J. Z. Zhang, L. J. Terminello, T. van Buuren, *ACS Nano* **2009**, 3, 325.

[23] M. Kuno, D. P. Fromm, H. F. Hamann, A. Gallagher, D. J. Nesbitt, *The Journal of Chemical Physics* **2000**, 112, 3117.

[24] N. Song, H. Zhu, S. Jin, W. Zhan, T. Lian, *ACS Nano* **2011**, 5, 613.

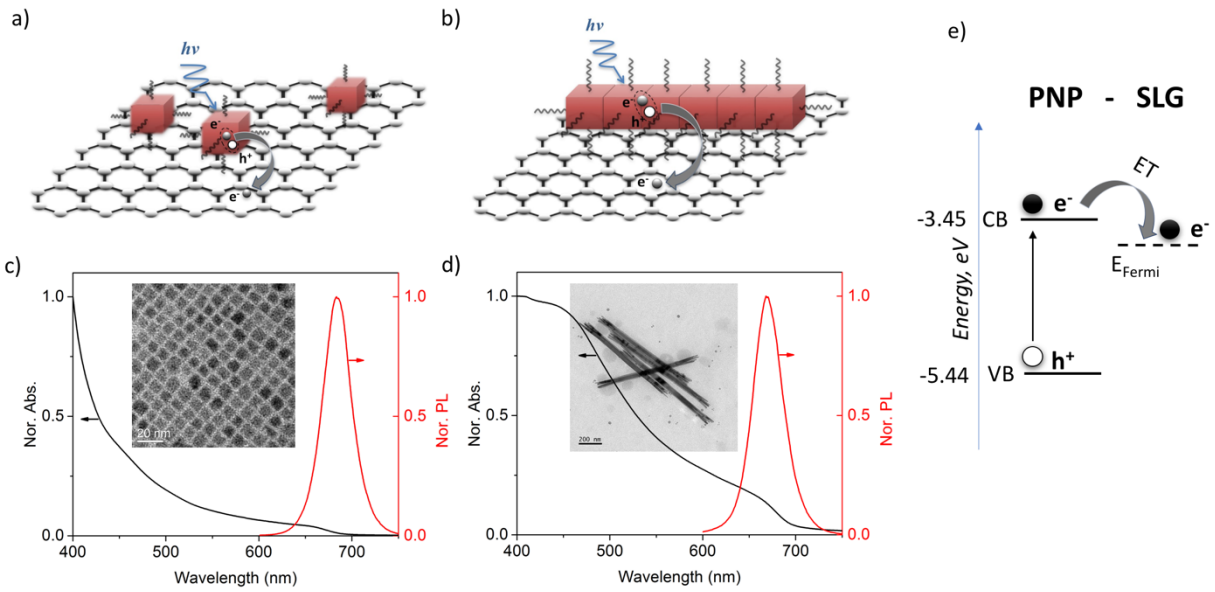

Figure 1. (a) and (b) are conceptual drawings of 0D-2D and 1D-2D hybrids based on perovskite nanocrystals and SLG and perovskite nanowire and SLG, respectively. (c) and (d) are optical absorption and PL emission spectra of $CsPbI_3$ perovskite nanoparticles (PNP) and nanowires (PNWs) in hexane. Insets are TEM images of perovskite nanocrystals (panel b) and nanowires (panel d). (e) band diagram with CB and VB values of $CsPbI_3$ nanocrystals from reference.[6]

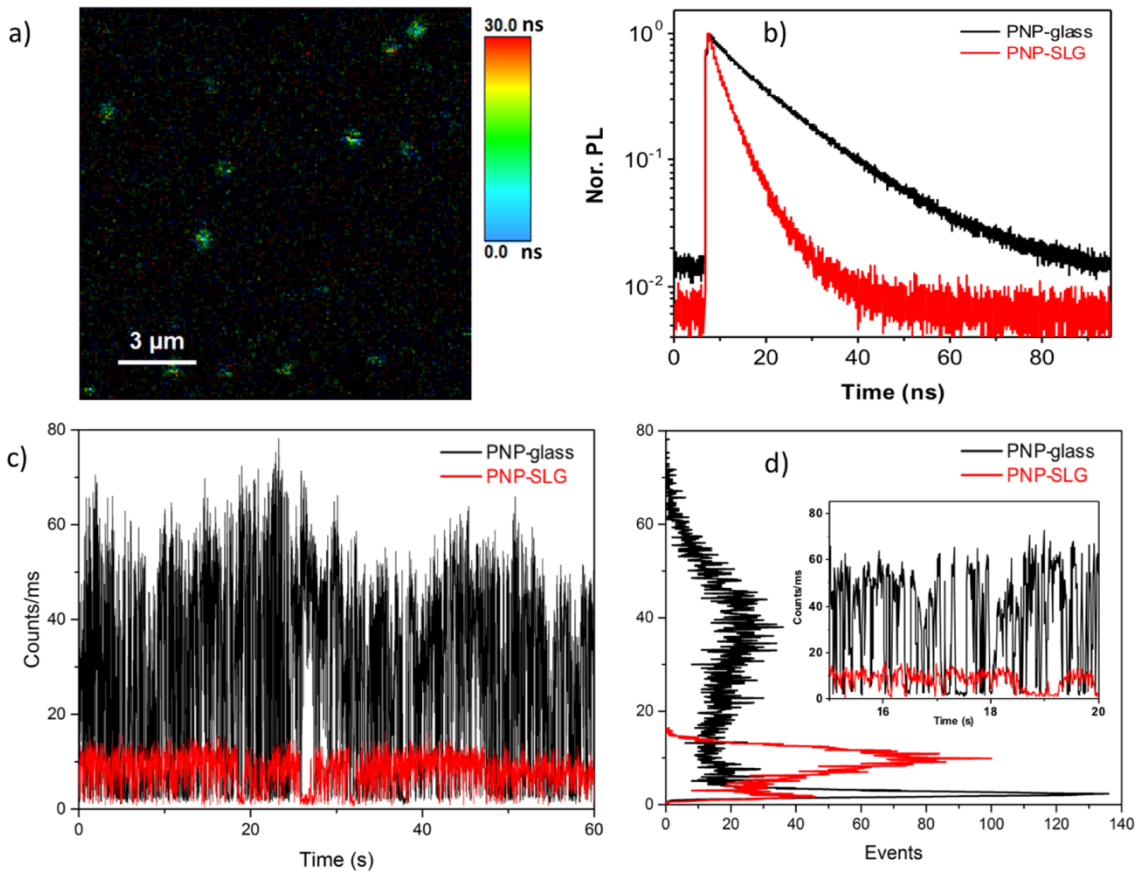

Figure 2. a) Confocal fluorescence lifetime image (FLIM) of isolated $CsPbI_3$ PNPs on cover glass and under inert gas atmosphere (excitation 440nm, 10 MHz, 100nW average power). Scale bar is 3 µm (b) PL decays from isolated $CsPbI_3$ PNPs on glass (black color, 13.36ns) and on single layer graphene (SLG, red color, 4.82ns). (c) Time trajectory of PL intensity and (d) associated photon counting histograms for isolated $CsPbI_3$ PNPs on cover glass (black color) and on SLG (red color). The inset in panel (d) is a zoom of the trace shown in panel (c) to visually demonstrate that no significant changes in photoluminescence blinking are observed from glass to SLG except drop in photon count rate.

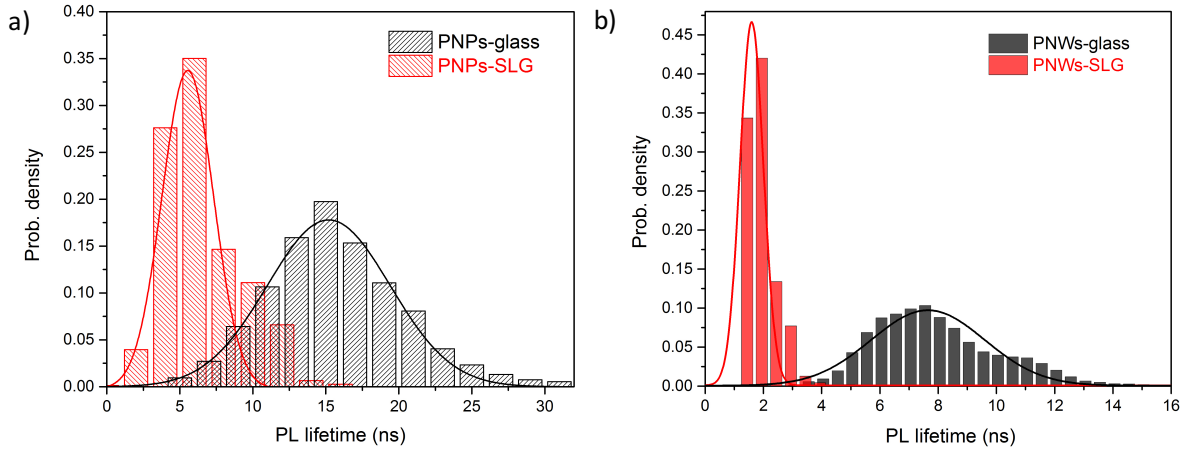

Figure 3. Normalized probability distributions of PL lifetimes and Gauss fits for a) PNPs on glass (black colors) and SLG (red colors) and for b) PNWs on glass (black colors) and SLG (red colors).

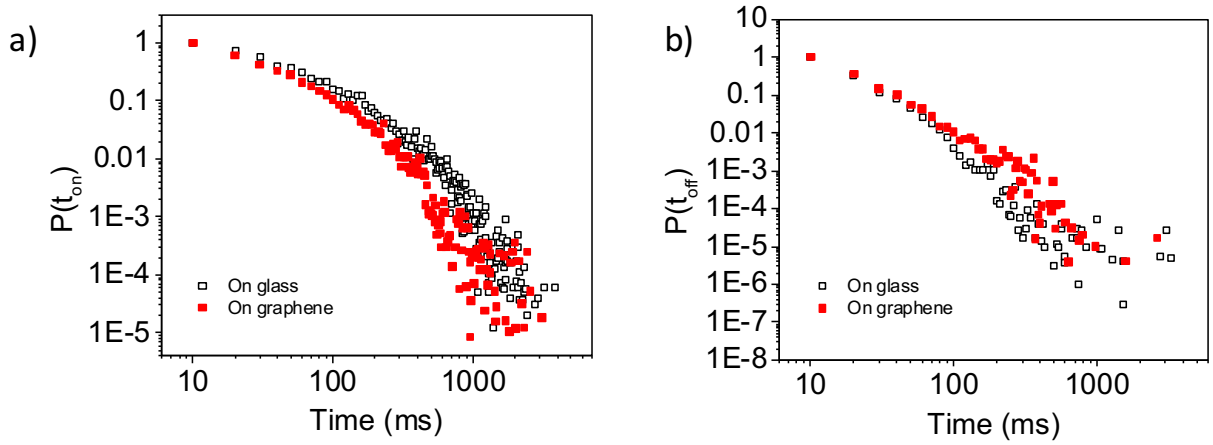

Figure 4. Photoluminescence blinking in isolated PNPs deposited on glass and on SLG. (a) on-time and (b) off-time probability distribution for PNPs on glass (black squares) and PNPs on SLG (red squares).

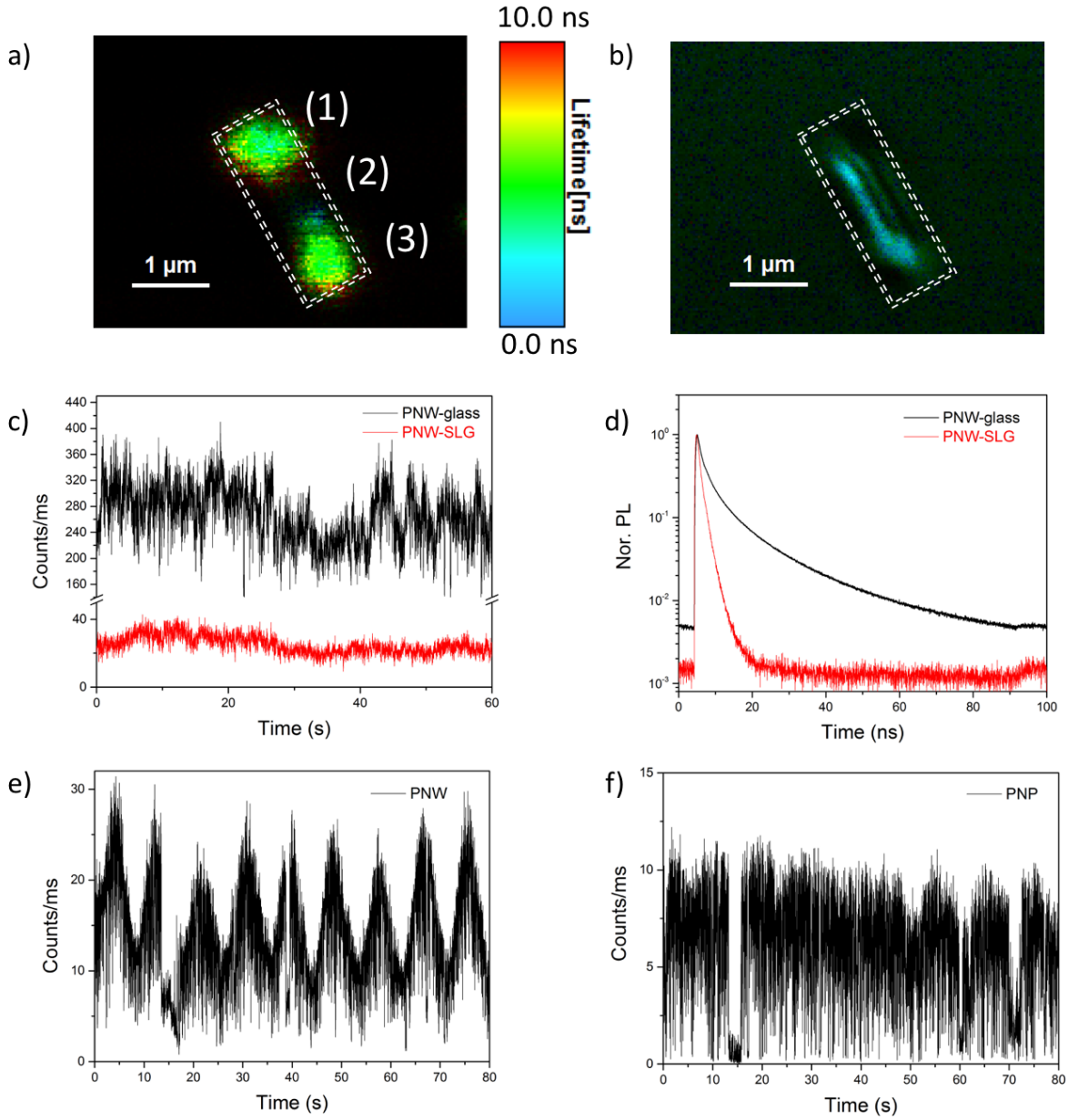

Figure 5. Correlative confocal FLIM (a) and back-scattering reflection (b) images of an isolated $CsPbI_3$ perovskite nanowire (PNW) on glass. c) PL intensity vs time trajectories from isolated PNWs on glass (black color) and on SLG (red color). d) PL decays from isolated PNWs on glass (black color, $< \tau_{PNW} >= 7.21$ ns) and on SLG (red color, $< \tau_{PNW-SLG} >= 1.20$ ns). (e) and (f) are PL intensity vs time trajectories from isolated PNW and PNP on glass following modulated polarized laser excitation.

Table 1. Photophysical parameters for pristine PNPs and PNWs and for 0D-2D and 1D-2D nanohybrids.

Sample	τ_{PL}/ns	FWHM $(\tau_{PL})/ns$	k_{ET} $x10^8 s^{-1}$	$E_{ET}(\%)$	m_{on}	m_{off}
PNP	15.2±0.13	9.9±0.38	-	-	1.46±0.03	1.82±0.02
PNW	7.65±0.05	4.6±0.13	-	-	-	-
PNP-SLG	5.54±0.25	4.2±0.7	1.14	64	1.62±0.04	1.67±0.02
PNW-SLG	1.58±0.01	0.95±0.03	5.06	79	-	-

TOC entry

Doping of poorly absorbing, highly conductive single layer graphene with perovskite nanocrystals and nanowires provides a simple and efficient path to obtain hybrids with increased light harvesting properties and improved exciton production for next generation photodetectors.

Keyword perovskite nanocrystals and nanowires, single layer graphene, electron transfer, single nanocrystal spectroscopy, blinking, photodetector devices.

Jia-Shiang Chen,[1,2] Tennyson L. Doane,[3] Mingxing Li,[1] Huidong Zang,[1] Mathew M. Maye,[3*] and Mircea Cotlet[1*]

0D-2D and 1D-2D semiconductor hybrids composed of all inorganic perovskite nanocrystals and single layer graphene with improved light harvesting
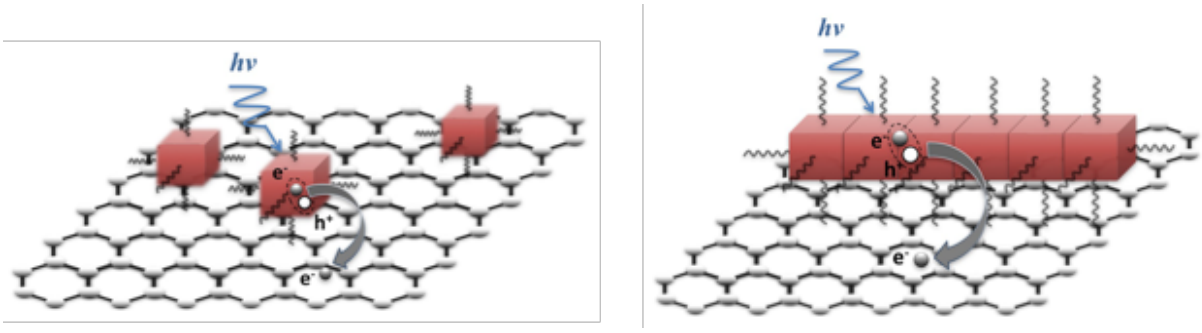
TOC figure